https://doi.org/10.5194/acp-2019-666
Preprint. Discussion started: 7 August 2019

Atmospheric Chemistry and Physics Discussions

Mechanistic Study of Formation of Ring-retaining and Ring-opening Products from Oxidation of Aromatic Compounds under Urban Atmospheric Conditions

Alexander Zaytsev[1], Abigail R. Koss[2], Martin Breitenlechner[1], Jordan E. Krechmer[3], Kevin J. Nihill[2], Christopher Y. Lim[2], James C. Rowe[2], Joshua L. Cox[4], Joshua Moss[2], Joseph R. Roscioli[3], Manjula R. Canagaratna[3], Douglas R. Worsnop[3], Jesse H. Kroll[2], and Frank N. Keutsch[1,4,5]

[1]John A. Paulson School of Engineering and Applied Sciences, Harvard University, Cambridge, MA 02138, USA,
[2]Department of Civil and Environmental Engineering, Massachusetts Institute of Technology, Cambridge, MA 02139, USA,
[3]Aerodyne Research Inc., Billerica, MA 01821, USA,
[4]Department of Chemistry and Chemical Biology, Harvard University, Cambridge, MA 02138, USA,
[5]Department of Earth and Planetary Sciences, Harvard University, Cambridge, MA 02138, USA

Correspondence to: Alexander Zaytsev (zaytsev@g.harvard.edu) and Frank N. Keutsch (keutsch@seas.harvard.edu)

Abstract. Aromatic hydrocarbons make up a large fraction of anthropogenic volatile organic compounds and contribute significantly to the production of tropospheric ozone and secondary organic aerosol (SOA). A series of toluene and 1,2,4-trimethylbenzene (1,2,4-TMB) photooxidation experiments were performed in an environmental chamber under relevant polluted conditions (NO_x ~ 10 ppb). An extensive suite of instrumentation including two Proton-Transfer Reaction Mass-Spectrometers (PTR-MS) and two Chemical Ionization Mass-Spectrometers (NH_4^+ CIMS and I^- CIMS) allowed for quantification of reactive carbon in multiple generations of oxidation. Hydroxyl radical (OH)-initiated oxidation of both species produces ring-retaining products such as cresols, benzaldehydes, and bicyclic intermediate compounds, as well as ring scission products such as epoxides, and dicarbonyls. We show that the oxidation of bicyclic intermediate products leads to formation of compounds with high oxygen content (O:C ratio up to 1.1). These compounds, previously identified as highly oxygenated molecules (HOMs), are produced by more than one pathway with differing numbers of reaction steps with OH, including both autooxidation and phenolic pathways. We report the elemental composition of these compounds formed under relevant urban high-NO conditions. We show that ring-retaining products for these two precursors are more diverse and abundant than predicted by current mechanisms. We present speciated elemental composition of SOA for both precursors and confirm that highly oxygenated products make up a significant fraction of SOA. Ring scission products are also detected in both the gas and particle phases, and their yields and speciation overall agree with the kinetic model prediction.

https://doi.org/10.5194/acp-2019-666
Preprint. Discussion started: 7 August 2019

Atmospheric Chemistry and Physics Discussions

1 Introduction

Aromatic compounds represent a significant fraction of volatile organic compounds (VOCs) in the urban atmosphere and play a substantial role in the formation of tropospheric ozone and secondary organic aerosol (SOA) (Calvert et al., 2002). Typical anthropogenic sources include vehicle exhaust, solvent use, and evaporation of gasoline and diesel fuels. Toluene, the most abundant alkylbenzene in the atmosphere, is primarily emitted by aforementioned anthropogenic processes. Toluene-derived SOA is estimated to contribute approximately 17-29% of the total SOA produced in urban areas (Hu et al., 2008). More highly substituted aromatic compounds make up another important group of aromatic compounds as they tend to have high SOA yields (Li et al., 2016) and account for a significant fraction of non-methane hydrocarbons in the industrialized regions of China (Tang et al., 2007; Zheng et al., 2009). 1,2,4-trimethylbenzene (1,2,4-TMB) serves as a model molecule to study oxidation of more substituted aromatic compounds.

In the atmosphere, oxidation of aromatic hydrocarbons is most often initiated by their reactions with hydroxyl radicals (OH) via H-abstraction from the alkyl groups or OH addition to the aromatic ring (Fig. 1) (Calvert et al., 2002). The abstraction channels are relatively minor, leading to the formation of benzyl radicals and benzaldehyde with yields of ~0.07 in the case of toluene (Wu et al., 2014) and ~0.06 in the case of 1,2,4-TMB (Li and Wang, 2014). The OH-adducts can react with atmospheric O_2 through H-abstraction to form ring-retaining phenolic compounds (i.e., cresols and trimethylphenols). The phenol formation yield decreases for the more substituted aromatics: in case of toluene the cresol yield is ~0.18 (Klotz et al., 1998, Smith et al., 1998) while for 1,2,4-TMB the trimethylphenol yield is ~0.03 (Bloss et al., 2005). Both abstraction and phenolic channels lead to the formation of products retaining the aromatic ring.

The OH-adducts can also react with O_2 through recombination. In this case they lose aromaticity and form non-aromatic ring-retaining bicyclic peroxy radicals (BPRs). Under low-NO conditions, BPRs react with HO_2 and RO_2, forming bicyclic hydroperoxides and bicyclic carbonyls, respectively (Fig. 2). In addition, BPRs can undergo unimolecular H-migration followed by O_2-addition (so-called autooxidation) leading to the formation of non-aromatic ring-retaining highly oxygenated organic molecules (HOMs) (Bianchi et al., 2019). Molteni et al. (2018) reported elemental composition of the HOMs from a series of aromatic compounds produced under low-NO conditions. The autooxidation pathway might be more important for the substituted aromatics because of the higher yield of BPR formation and the larger number of relatively weak C-H bonds (Wang et al., 2017). Under urban-relevant high-NO conditions BPRs also react with NO to form bicyclic oxy radicals that decompose to ring scission carbonylic products such as (methyl) glyoxal and biacetyl. Recent theoretical studies predict a new type of epoxy-dicarbonyl products that have not reported in previous studies (Li and Wang, 2014, Wu et al., 2014). Reaction of BPRs with NO can also result in formation of bicyclic organonitrates. Both ring-retaining and ring scission compounds are expected to be low in volatility and contribute significantly to SOA (Schwantes et al., 2017). There remain a number of major uncertainties in model representation of oxidation of aromatic compounds including overprediction of ozone concentration, underprediction of OH production and lack of detailed description of SOA formation (Birdsall and Elrod, 2011; Wyche et al., 2009).

https://doi.org/10.5194/acp-2019-666
Preprint. Discussion started: 7 August 2019

Atmospheric Chemistry and Physics Discussions

In the present work, we investigate the detailed mechanism of hydroxyl radical multigeneration oxidation chemistry of two aromatic hydrocarbons: toluene and 1,2,4-trimethylbenzene under moderate, urban-relevant NO_x levels (~10 ppbv). Laboratory experiments were conducted at an environmental chamber over approximately 1 day of atmospheric-equivalent oxidation. We use four high-resolution time-of-flight chemical ionization mass spectrometers (NH_4^+ CIMS, I^- CIMS and two PTR-MS) to characterize and quantify gas- and particle-phase oxidation products. We identify gas-phase pathways leading to production of low-volatility compounds which are important for SOA formation and support these identifications with CIMS data and a method to characterize the kinetics of an oxidation system.

2 Methods

2.1 Experimental design

All experiments were performed in a 7.5 m^3 Teflon environmental chamber (Hunter et al., 2014). Prior to experiments, the chamber was flushed and filled with purified air. During experiments clean air was continuously added to the chamber to keep its volume constant. The temperature of the chamber was controlled at 292 K and approximately 2% relative humidity.

We performed a series of photochemical experiments, in which toluene and 1,2,4-TMB were oxidized by OH under high-NO conditions (Table S1). First, dry ammonium sulfate particles, used as condensation nuclei, were injected in the chamber to reach a number concentration of 2.5-5.7·10^4 cm^{-3}. Seed particles were not injected into the chamber in two experiments. Hexafluorobenzene, (C_6F_6, which serves as a dilution tracer) was then added to the chamber. Nitrous acid (HONO) was later injected as an OH precursor. HONO was generated in a bubbler containing a solution of sodium nitrite by adding 2-4 μL of sulfuric acid via a syringe pump. 15 lpm of subsequently injected purified air carried HONO into the chamber, which resulted in a concentration of 35-45 ppbv. The concentration of NO in the chamber was estimated to be ~0.3 ppbv while NO_2 concentration was approximately 10 ppbv. After the addition of the oxidant, the aromatic precursor (toluene or 1,2,4-TMB, Sigma-Aldrich) was added to the chamber by injecting 3 μL of the precursor into a heated inlet. The initial concentration of the precursor was 89 ppbv in toluene experiments and 69 ppbv in 1,2,4-TMB experiments. The reagents were allowed to mix for several minutes, after which the ultraviolet (UV) lights, centred ~340 nm, were turned on to start photolysis of HONO and photooxidation of the precursor. During experiments, additional injections of HONO were added to the chamber in order to roughly maintain the OH levels. Measurements were conducted within several hours, which corresponds to 14-16 hours of atmospheric-equivalent exposure (assuming an average OH concentration of 1.5·10^6 molecules cm^{-3}). Concentrations of O_3 and HONO+NO_x for a typical run are shown on Fig S1.

2.2 Chamber instrumentation

The concentration of nitrogen oxides (NO_x) and HONO (42i NO_x monitor, Thermo Fisher Scientific), ozone (2B Technologies), relative humidity, and temperature were measured in the chamber. Aromatic precursors as well as gas-phase oxygenated volatile organic compounds (OVOCs) were detected by chemical ionization high-resolution time-of-flight mass

https://doi.org/10.5194/acp-2019-666
Preprint. Discussion started: 7 August 2019

Atmospheric Chemistry and Physics Discussions

spectrometry (CIMS) instruments, including the I^- CIMS instrument (Aerodyne Research Inc.; Lee et al., 2014) and two proton-transfer-reaction mass-spectrometry (PTR-MS) instruments: Vocus-2R-PTR-TOF (TOFWERK A.G.; Krechmer et al., 2018) and PTR3 (Ionicon Analytik; Breitenlechner et al., 2017). The latter instrument was operated in a switching-mode regime using $H_3O^+ \cdot (H_2O)_n$, n=0-1 (as H_3O^+ CIMS) and $NH_4^+ \cdot (H_2O)_n$, n = 0-2 (as NH_4^+ CIMS) primary ions (Hansel et al., 2018; Zaytsev et al., 2019). Switching between ion modes occurred every five minutes. Each CIMS instrument used a 3/16'' PFA Teflon sampling line of 1 m in length with a flow of 2 slm. PTR3 and Vocus-2R-PTR-TOF are designed to minimize inlet losses of sampled compounds (Krechmer et al., 2018; Breitenlechner et al., 2017). Detection efficiency and sensitivity of CIMS instruments depend critically on both the reagent ion and the measured sample molecule. The concentrations of aromatic precursors were measured by Vocus-2R-PTR-TOF, which was directly calibrated for the two compounds. Smaller, less oxidized molecules were primarily quantified by PTR-MS (PTR3 H_3O^+ CIMS and Vocus-2R-PTR-TOF) while PTR3 NH_4^+ CIMS and I^- CIMS were mainly used for detection of larger and more functionalized molecules. PTR3 and I^- CIMS instruments were directly calibrated for 10 VOCs with various functional groups. An average calibration factor was applied to other species detected by PTR-MS instruments, while collision-dissociation methods were implemented to constrain sensitivities of I^- CIMS and NH_4^+ CIMS (Lopez-Hilfiker et al., 2016; Zaytsev et al., 2019). Use of these methods and average calibration factors leads to uncertainties in estimated concentrations of detected compounds within a factor of ten. NH_4^+ CIMS uncertainties are within a factor of three while I^- CIMS is less certain. The majority of analysis in this work relies on NH_4^+ CIMS and PTR-MS data while I^- CIMS data are used as supporting measurements. CO and formaldehyde were measured by tunable infrared laser differential absorption spectroscopy (TILDAS; Aerodyne Research Inc.), and glyoxal was detected by laser induced phosphorescence (Madison LIP; Huisman et al., 2008).

Total organic aerosol mass was measured using an Aerodyne Aerosol Mass Spectrometer (AMS, DeCarlo et al., 2006), calibrated with ammonium nitrate and assuming a collection efficiency of 1. Particle-phase compounds were quantified using the FIGAERO-HRToF-I^-CIMS (Lopez-Hilfiker et al., 2014), and a second PTR3 that could be operated in two positive modes as described above and equipped with an aerosol inlet comprising a gas-phase denuder and a thermal desorption unit (TD-NH_4^+ CIMS and TD-H_3O^+ CIMS) (Zaytsev et al., 2019).

2.3 Kinetic model

The Framework for 0-D Atmospheric Modelling v3.1 (F0AM; Wolfe et al., 2016) containing reactions from the Master Chemical Mechanism (MCM v3.3.1) (Jenkin et al., 2003; Bloss et al., 2005) was used to simulate photooxidation of 1,2,4-TMB and toluene in the environmental chamber and to compare the modelled products with the measurements. Model calculations were constrained to physical parameters of the environmental chamber (pressure, temperature, photolysis frequencies and dilution rate calculated using the hexafluorobenzene tracer). Injections of aromatic compounds and HONO were modelled as sources during the time of injection, and the chamber lights intensity was tuned to match the measured time-dependent concentration of aromatic precursors with the modelled values. The chamber wall loss and dilution term for volatile compounds was estimated based on the concentration of the dilution tracer, hexafluorobenzene. As for semi- and low-volatile

https://doi.org/10.5194/acp-2019-666
Preprint. Discussion started: 7 August 2019

Atmospheric Chemistry and Physics Discussions

compounds, the wall deposition rate was estimated to be $5 \cdot 10^{-4}$ s^{-1} using the "rapid burst" method described in detail by Krechmer et al. (2016).

2.4 Calculation of OH exposure and product yields

The OH concentration was determined using the decay of the aromatic precursor, accounting for losses from dilution and chamber wall deposition. The mixing ratio of the aromatic VOC (ArVOC: toluene or 1,2,4-TMB) is given by the following kinetics equation:

$$[\mathrm{ArVOC}]_t = [\mathrm{ArVOC}]_0 \cdot \exp(-k_{\mathrm{ArVOC+OH}} \cdot [\mathrm{OH}_{\mathrm{exposure}}]_t - k_{\mathrm{physical\ loss\ ArVOC}} \cdot t) \quad (1)$$

where [ArVOC] is the time-dependent mixing ratio of the aromatic precursor, $k_{\mathrm{ArVOC+OH}}$ is the second-order rate constant for ArVOC + OH reaction ($k_{\mathrm{toluene+OH}}$ = $5.63 \cdot 10^{-12}$ cm^3 $molecule^{-1}$ s^{-1} and $k_{1,2,4-\mathrm{TMB+OH}}$ = $3.25 \cdot 10^{-11}$ cm^3 $molecule^{-1}$ s^{-1} at 293K (Calvert et al., 2002)), $[\mathrm{OH}_{\mathrm{exposure}}]_t = \int_o^t [\mathrm{OH}] d\tau$ is the integrated OH exposure, $k_{\mathrm{physical\ loss\ ArVOC}}$ is the unimolecular rate constant determining dilution and chamber wall loss, and *t* is the time since the beginning of irradiation by the UV lights.

Yields of first-generation products were determined based on the decay of the aromatic precursor, rise of the product, and accounting for physical (dilution and chamber wall deposition) and chemical losses (reaction with OH, NO_3, O_3 and photolysis). A correction procedure described in detail by Galloway et al. (2011) is applied to calculate product yields. This correction takes into account physical and chemical losses of products in the environmental chamber:

$$[\mathrm{X}]_i^{\mathrm{corr}} = [\mathrm{X}]_{i-1}^{\mathrm{corr}} + \Delta[\mathrm{X}]_i + [\mathrm{X}]_{i-1} \Delta t (k_{\mathrm{chemical\ loss}} + k_{\mathrm{physical\ loss}}) \quad (2)$$

where $[\mathrm{X}]_i^{\mathrm{corr}}$ is the corrected mixing ratio of the compound at measurement time *i*, Δt is time between measurements *i* and *i* – 1, $[\mathrm{X}]_{i-1}$ is the measured product mixing ratio of measurement *i* – 1, $\Delta[\mathrm{X}]_i$ is the observed net change in [X] that occurs over Δt, $k_{\mathrm{chemical\ loss}}$ and $k_{\mathrm{physical\ loss}}$ are the rate constants describing chemical and losses of the product.

Yields of first-generation products were determined from the linear relationship between the amount of the corrected product formed and the amount of the primary ArVOC reacted:

$$[\mathrm{X}]^{\mathrm{corr}} = Y[\mathrm{ArVOC}]^{\mathrm{reacted}} + b \quad (3)$$

where $[\mathrm{X}]^{\mathrm{corr}}$ is the amount of the corrected product formed, $[\mathrm{ArVOC}]^{\mathrm{reacted}}$ is the amount of the primary ArVOC reacted and *Y* is the first-generation yield of the product.

2.5 Gamma kinetics parameterization

Photooxidation products can be characterized not only by their concentration and yield, but also by their time series behaviour. In a laboratory experiment, the time series behaviour of a product is dependent on the kinetic parameters of the molecule: the relative rates of formation and reactive loss, and the number of reactions to create the product. We characterize time series behaviour of products using the gamma kinetics parametrization (GKP), which describes kinetics of an oxidation system in terms of multigenerational chemistry. The detailed description of this parametrization technique is given by Koss et al. (2019),

https://doi.org/10.5194/acp-2019-666
Preprint. Discussion started: 7 August 2019

Atmospheric Chemistry and Physics Discussions

so we include only a brief description here. A multigenerational hydroxyl radical oxidation system can be represented as a linear system of reactions:

$$X_0 \xrightarrow{k\cdot[OH]} X_1 \xrightarrow{k\cdot[OH]} X_2 \xrightarrow{k\cdot[OH]} \dots \xrightarrow{k\cdot[OH]} X_m \xrightarrow{k\cdot[OH]} X_{m+1} \xrightarrow{k\cdot[OH]} \dots \quad (4)$$

where k is the second-order rate constant and m is the number of reactions needed to produce species X_m.

In laboratory experiments, oxidation reactions can be parametrized as a linear system of first-order reactions if reaction time t is replaced by OH exposure $[OH_{exposure}]_t = \int_0^t [OH] d\tau$. In this case, the time-dependent concentration of a compound X_m can be parametrized by (Koss et al., 2019):

$$[X_m](t) = a(k \cdot [OH_{exposure}]_t)^m e^{-k\cdot[OH_{exposure}]t} \quad (5)$$

where a is a scaling factor, k is the effective second-order rate constant (cm^3 molecule^{-1} s^{-1}), m is the generation number, and $[OH_{exposure}]_t$ is the integrated OH exposure (molecule s cm^{-3}).

Eq. (5) can be used to fit the observed concentration of a compound to return its parameters a, k and m. The parameter m determines the number of reactions with OH needed to produce the compound while the parameter k gives an approximate measure of the compound reactivity. We define "generation" here as the number of reactions with OH. Examples of fitted chamber measurements are shown in Fig. S2.

3 Results and discussion

Toluene and 1,2,4-TMB react with OH to form both ring-retaining (via benzaldehyde, phenolic and bicyclic channels) and ring scission (via bicyclic and epoxide channels) products. (The toluene oxidation scheme from MCM v3.3.1 is shown on Fig. 1.) First and later-generation gas- and particle-phase oxidation products are detected and quantified for both systems. In the following sections we compare products suggested by MCM and previous studies to corresponding molecular formulas detected by CIMS. In some cases, the ion identity is well established from previous research or because there are a limited number of reasonable structures (e.g., phenols, benzaldehydes and ring-scission dicarbonyl products); in other cases, multiple isomers are possible, which could contribute to some differences between modelled and observed behaviour.

3.1 Products from benzaldehyde, phenolic and epoxide channels

In the toluene experiments, the approximate yields of benzaldehyde and cresol (~0.10 and ~0.16 correspondingly) were calculated based on the decay of toluene measured by Vocus-2R-PTR-TOF, rise of the two products measured by PTR3 H_3O^+ CIMS and NH_4^+ CIMS, and accounting for losses of cresol and benzaldehyde from wall deposition and reaction with OH and NO_3 (Sect 2.4). MCM v3.3.1 recommends a 0.07 yield of benzaldehyde and a 0.18 yield of cresol (total of all isomers) from OH initiated oxidation of toluene. Benzaldehyde and cresol concentrations predicted by MCM agree within uncertainties with the PTR3 H_3O^+ CIMS and NH_4^+ CIMS measurements and the time-series behaviour of measurements and model predictions are similar (Fig. 3a). In general, MCM predicts that phenolic and benzaldehyde channels are less important for more substituted

https://doi.org/10.5194/acp-2019-666
Preprint. Discussion started: 7 August 2019

Atmospheric Chemistry and Physics Discussions

aromatics (Bloss et al., 2005). Hence, the kinetic model recommends a 0.06 yield of dimethylbenzaldehyde and a 0.03 yield of trimethylphenol from the OH-initiated oxidation of 1,2,4-TMB. The model predictions for the two products agree within uncertainties with the PTR-MS measurements and the time series behaviour is again similar (Fig. 3b). Phenols and benzaldehydes can further react within the MCM v3.3.1 scheme to form highly oxidized second-generation compounds. The importance of this pathway is discussed further in section 3.2.1.

MCM v3.3.1 also includes an epoxy-oxy channel in which it predicts formation of non-fragmentary linear epoxide-containing products (Fig. 1). The predicted yields of these species are 0.10 and 0.30 for toluene and 1,2,4-TMB systems, respectively. The observed yields of these products are significantly smaller (~0.01 in both systems). The observations are however consistent with theoretical studies (Li and Wang, 2014; Wu et al., 2014) in which it has been shown that only a negligible fraction of the bicyclic radicals would break the -O-O- bond to form epoxide-containing products.

3.2 Products from bicyclic pathway

3.2.1 Non-fragmented, ring-retaining products

Bicyclic peroxy radicals (BPRs) are formed through the addition of O_2 to the OH-adducts (Fig. 1). Starting from a generic aromatic compound C_xH_y, we expect the formation of BPRs with the formula $C_xH_{y+1}O_5$. BPRs likely react with RO_2, HO_2, or NO leading to the following products (Fig. 2) (Birdsall and Elrod, 2011): bicyclic carbonyls ($C_xH_yO_4$), bicyclic alcohols ($C_xH_{y+2}O_4$), bicyclic hydroperoxides ($C_xH_{y+2}O_5$), and bicyclic organonitrates ($C_xH_{y+1}NO_6$), as well as alkoxy radicals (discussed later). A number of oxygenated products is detected by NH_4^+ CIMS including $C_7H_8O_4$, $C_7H_{10}O_5$ and $C_7H_9NO_6$ in the toluene experiments, and $C_9H_{12}O_4$, $C_9H_{14}O_4$ and $C_9H_{13}NO_6$ in the 1,2,4-TMB experiments (Table 3). Since authentic standards are not available, quantification of these compounds was done using a voltage scanning procedure based on collision-induced dissociation (Sect. 2.2). The majority of OVOCs with high carbon numbers were detected at the maximum sensitivity, which was experimentally determined in each photooxidation experiment and depends on operational conditions of the NH_4^+ CIMS instrument (Zaytsev et al., 2019) (Tables S2 and S3). A number of products with the same molecular formulas corresponding to bicyclic carbonyls ($C_7H_8O_4$ and $C_9H_{12}O_4$) and alcohols ($C_7H_{10}O_4$ and $C_9H_{14}O_4$) were also detected by I^- CIMS and PTR-MS.

In MCM v3.3.1, the bicyclic peroxy radical undergoes analogous reactions: (1) it can react with HO_2 producing a hydroperoxide; (2) it can react with RO_2 producing an alkoxy radical, an alcohol or a carbonyl; (3) it can react with NO producing an alkoxy radical or a nitrate. According to MCM, under relevant urban conditions BPRs nearly exclusively react with NO and HO_2 and dominantly form alkoxy radicals which further decompose to smaller ring scission compounds (Figs. 2, S3 and S4) (Sect. 3.2.3). In this study, the estimated lifetime of BPRs, calculated as inverse reactivity, is estimated to be ~5 s for toluene and ~7 s for 1,2,4-TMB. MCM v3.3.1 does not include formation of the bicyclic carbonyl, $C_9H_{12}O_4$, in the 1,2,4-TMB oxidation scheme, while in the case of toluene it predicts that a major fraction of bicyclic carbonyl $C_7H_8O_4$ is produced as a second-generation product from the reaction of bicyclic hydroperoxide and organonitrate with OH. In contrast, the GKP

https://doi.org/10.5194/acp-2019-666
Preprint. Discussion started: 7 August 2019

Atmospheric Chemistry and Physics Discussions

fit based on the NH_4^+ CIMS measurements implies that a significant fraction of detected compounds is formed in the first generation in both systems (Table 3). These first-generation bicyclic carbonyls can be produced by the reaction of BPR with HO_2 or RO_2. In addition, MCM significantly underestimates the concentration of bicyclic alcohol ($C_9H_{14}O_4$ for 1,2,4-TMB system) since the only channel present in the model is a reaction of BPR with RO_2 while it can also be produced via the BPR+HO_2 pathway (Fig. 2). Finally, MCM v3.3.1 predicts that a notable fraction of BPR reacts with HO_2 to form bicyclic hydroperoxide. NH_4^+ CIMS measurements of $C_9H_{14}O_5$ and $C_7H_{10}O_5$ are less than the model prediction for each chemical system but agree within measurement uncertainties. The generation number *m* of $C_7H_{10}O_5$ and $C_9H_{14}O_5$ is ~1.7-1.8 which suggests that a compound with the same molecular formula can be produced by more than one pathway with different number of reaction steps. Birdsall and Elrod (2011) proposed that the BPR from several aromatic precursors reacting with HO_2 can form an alkoxy radical and OH. Similarly, recent studies have shown that numerous peroxy radicals do not form a hydroperoxide in unity yield while reacting with HO_2 (Praske et al., 2015; Orlando and Tyndall, 2012). Hence, we observe formation of numerous highly oxygenated compounds with molecular formula corresponding to bicyclic carbonyls, alcohols, organonitrates, and hydroperoxides via the peroxide-bicyclic channel under high-NO conditions.

In addition to the formation of closed-shell products, bicyclic peroxy radicals can undergo isomerization reactions to form more oxidized peroxy radicals (Fig. 2) (Wang et al., 2017; Molteni et al., 2018). These reactions are not included in MCM v3.3.1. These radicals can in turn react with RO_2, HO_2, or NO leading to a series of more oxidized bicyclic products, so-called highly oxygenated molecules (HOMs): carbonyl ($C_xH_yO_6$), alcohol ($C_xH_{y+2}O_6$), hydroperoxide ($C_xH_{y+2}O_7$), and nitrate ($C_xH_{y+1}NO_8$). Several products with the aforementioned molecular formulas are detected by NH_4^+ CIMS (Fig. 4). In the toluene experiments, $C_7H_8O_6$, $C_7H_{10}O_6$, and $C_7H_9NO_8$ were detected by NH_4^+ CIMS as $(NH_4^+)\cdot$OVOC. In the 1,2,4-TMB experiments, $C_9H_{14}O_6$, and $C_9H_{13}NO_8$ were detected as $(NH_4^+)\cdot$OVOC while $C_9H_{12}O_6$ was detected both as $(NH_4^+)\cdot C_9H_{12}O_6$ (m/z 234.098) and as $[(NH_4)\cdot(H_2O)\cdot C_9H_{12}O_6]^+$ (m/z 252.108). The yield of molecules with a high O:C (greater than 0.44) ratio is larger in the case of 1,2,4-TMB compared to toluene. However, the gamma kinetics parametrization suggests that none of these compounds are solely first-generation products (Table 3) which implies that there are multiple chemical pathways in which products with the same molecular formula (but potentially different structure) are formed. Some of the products can be produced in the bicyclic oxidation pathway of cresol or trimethylphenol resulting in formation of alcohols ($C_xH_{y+2}O_5$), hydroperoxides ($C_xH_{y+2}O_6$) and nitrates ($C_xH_{y+1}NO_7$). Formation of bicyclic alcohols and hydroperoxides from the phenolic channel is included in MCM v3.3.1. We conclude that although a plethora of compounds with a high O:C ratio was observed, only some of them are formed via first-generation isomerization/autooxidation pathways. These findings underline the importance of phenolic and benzaldehyde channels for producing highly oxygenated compounds especially for the less substituted aromatics given the high yields of phenols and benzaldehydes and their high reactivity.

3.2.2 Fragmented ring-retaining products

In addition to non-fragmented functionalized C_9 and C_7 products possibly formed via the bicyclic channel, a variety of lower-carbon containing (C_8 and C_6) products with fewer carbon atoms were also detected in both chemical systems. The total

https://doi.org/10.5194/acp-2019-666
Preprint. Discussion started: 7 August 2019

Atmospheric Chemistry and Physics Discussions

concentration of C_8 components predicted by MCM v3.3.1 for 1,2,4-TMB is in good agreement with the NH_4^+ CIMS and PTR-MS measurements, though the observed composition is distinctly different from the MCM prediction (Fig. 5). According to MCM, there are only four C_8 products with mixing ratios at or above the ppt level. The most abundant predicted compound, bicyclic carbonyl ($C_8H_{10}O_4$, MXYOBPEROH in MCM), is produced via the reaction of bicyclic nitrate $C_9H_{13}NO_6$ with OH, while the second most abundant compound, dimethylnitrophenol ($C_8H_9NO_3$, DM124OHNO2 in MCM), is formed in the benzaldehyde pathway. While all of the predicted products have been observed, NH_4^+ CIMS and PTR-MS also detect a plethora of C_8 compounds not included in MCM. Furthermore, MCM only predicts a total of 0.16 ppb for all C_6 compounds in the toluene experiments, while the combined measured mixing ratio of 15 C_6 compounds is ~0.5 ppb (Fig S5). The two most prominent C_6 products recommended by MCM, $C_6H_5NO_3$ and $C_6H_6O_2$, are predicted to be formed in the benzaldehyde channel. There are several pathways that may lead to the formation of the fragmented ring-retaining C_8 and C_6 products. One of them is ipso addition followed by dealkylation (Loison et al., 2012). In their study of the dealkylation pathway in the OH-initiated oxidation of several aromatic compounds, Noda et al. (2009) showed the importance of this pathway and reported dealkylation yields of 0.054 for toluene. Similarly, Birdsall and Elrod determined a 0.047 yield of dealkylation products for toluene. Loison et al. (2012) reported a 0.02 yield of dealkylation pathway products from the hexamethylbenzene + OH reaction. However, in some studies yields of dealkylation products have been found below 0.01 (Aschmann et al., 2010). While we cannot determine exact yields of observed dealkylation compounds since many of them are later-generation products, we estimate an overall amount of carbon of ~3 ppbC and ~5 ppbC stored in C_6 and C_8 compounds for toluene and 1,2,4-TMB, respectively, compared to 600 ppbC in the system as a whole. Although observed concentrations of these products are not very high, a significant fraction of them are highly oxygenated products with an O:C ratio greater than 0.5. These products can effectively partition to the particle phase and contribute to SOA formation (Section 3.3).

3.2.3 Products from ring scission pathway

Recent theoretical studies suggest that the ring scission pathway leads to a series of two ring scission products such that the total number of carbon atoms present in the original aromatic compound is conserved in the two products (Wu et al., 2014; Li and Wang, 2014). In particular, a toluene study by Wu et al. (2014) predicts significant yields of 1,2-dicarbonyls and a range of C_4 and C_5 products. Those larger compounds include dicarbonyls (butenedial $C_4H_4O_2$ and methylbutenedial $C_5H_6O_2$), which were already detected in previous experimental studies (Calvert et al., 2002), and newly proposed epoxy-dicarbonyl products (epoxybutanedial $C_4H_4O_3$ and methylepoxybutanedial $C_5H_6O_3$). As for 1,2,4-TMB, Li and Wang (2014) also predict two groups of ring scission products: (1) smaller 1,2-dicarbonyls such as glyoxal, methylglyoxal and biacetyl and (2) larger C_5, C_6 and C_7 products. Similar to the toluene system, those larger compounds include dicarbonyls ($C_5H_6O_2$, $C_6H_8O_2$ and $C_7H_{10}O_2$), which were previously reported in numerous studies, and new epoxy-dicarbonyl products ($C_5H_6O_3$ and $C_6H_8O_3$). Some experimental studies reported that larger ring scission products were found at systematically lower yields than the corresponding 1,2-dicarbonyl products (Arey et al., 2009). This result suggests that either the product pair carbon conservation

https://doi.org/10.5194/acp-2019-666
Preprint. Discussion started: 7 August 2019


Atmospheric Chemistry and Physics Discussions

rule is not followed or that the larger products undergo further photochemical or heterogeneous degradation in the environmental chamber.

A series of 1,2-dicarbonyls were experimentally detected including glyoxal and methylglyoxal in the toluene experiments, and methylglyoxal and biacetyl in the 1,2,4-TMB experiments (Tables 1 and 2). Although a relatively small amount of glyoxal (2.5 ppb) is predicted to be formed from the 1,2,4-TMB + OH pathway, observed amounts of glyoxal were below the limit of detection of the Madison LIP instrument (1 ppb) suggesting that the glyoxal yield does not exceed 0.03 in this system. Measured glyoxal and methylglyoxal formation yields, combined with the biacetyl yield from the 1,2,4-TMB oxidation, indicate that under high-NO conditions the first-generation yield of all 1,2-dicarbonyls is ~0.43 and ~0.35 for toluene and 1,2,4-TMB, respectively (Tables 1 and 2). For all 1,2-dicarbonyls the observed generation number *m* is greater than 1 and is consistent between the two systems, which suggests that these compounds are produced by more than one pathway with different numbers of reaction steps. In addition to the aforementioned 1,2-dicarbonyls, a series of dicarbonyls with a higher carbon number was observed in both systems (Tables 1 and 2). For all these species (except trimethylbutenedial) the generation number *m* is slightly smaller than 1. Finally, ions corresponding to newly proposed epoxy-dicarbonyl products were also observed (Tables 1 and 2). However, the generation number *m* for these compounds is between 1 and 2, suggesting that there are multiple pathways resulting in compounds with those molecular formulas. Overall, we observed ~0.45 and ~0.47 yields of larger carbonyls in the toluene and 1,2,4-TMB experiments, respectively.

3.3 SOA Analysis

Peak SOA concentration measured by TD-NH_4^+ CIMS was 1.8 μg m^{-3} for the toluene oxidation experiment and 1.4 μg m^{-3} for 1,2,4-TMB which is in good agreement with the AMS measurements (1.9 μg m^{-3} and 1.6 μg m^{-3}, respectively). Figure 6 depicts the relative distribution of carbon in the particle phase according to the carbon atom number n_C for 1,2,4-TMB and toluene SOA, respectively. The O:C ratios calculated from individual species measured from thermally desorbed SOA using NH_4^+ CIMS were ~0.95 for toluene SOA and ~0.7 for 1,2,4-TMB SOA. These ratios are in good agreement with the atomic O:C ratios measured by AMS (0.85 and 0.65 for toluene and 1,2,4-TMB SOA, respectively) (Canagaratna et al., 2015).

Products observed in the gas phase are compared to those detected in the particle phase to further understand the mechanism of SOA formation from aromatics precursors. A variety of ring-retaining products were observed in the particle phase for oxidation of 1,2,4-TMB and toluene: non-fragmentary products (e.g., $C_9H_{12}O_{4\text{-}6}$ for 1,2,4-TMB and $C_7H_8O_{4\text{-}6}$ for toluene) and fragmentary products (e.g., $C_8H_{10}O_{4\text{-}5}$, $C_7H_8O_{4\text{-}5}$ for 1,2,4-TMB and $C_6H_6O_{4\text{-}5}$ for toluene). The same non-fragmentary ring-retaining oxidation products, detected by NH_4^+ CIMS in the gas phase and expected to be low in volatility, are detected in the particle phase (Fig. 4). Overall, ring-retaining products make up a significant fraction of the total 1,2,4-TMB SOA mass (~25% for 1,2,4-TMB SOA and ~30% for toluene SOA) (Fig. 6), even though the total concentration of these products in the gas phase is relatively small (~2 ppb for 1,2,4-TMB and ~1 ppb for toluene). Furthermore, numerous masses corresponding to those of the ring scission products were detected including $C_5H_8O_3$, $C_4H_6O_3$, and $C_3H_4O_2$. It is likely that the concentration of larger ring-retaining products in the particle phase is underestimated due to their thermal fragmentation in the desorption unit

https://doi.org/10.5194/acp-2019-666
Preprint. Discussion started: 7 August 2019

Atmospheric Chemistry and Physics Discussions

inlet of the NH_4^+ CIMS instrument (Zaytsev et al., 2019) although it should be noted that many highly oxygenated compounds were detected, e.g., $C_7H_6O_6$ and $C_9H_{10}O_7$. These findings underscore the importance of bicyclic, phenolic and benzaldehyde channels for producing ring-retaining highly oxygenated compounds that comprise a significant fraction of SOA (more than 25%).

4 Conclusions and implications for the aromatic oxidation mechanism

In the present work, we studied the multigenerational photooxidation of two aromatic compounds (toluene and 1,2,4-trimethylbenzene) in an environmental chamber under relevant urban high-NO conditions. We identified a number of oxidation products based on their molecular formula and determined yields for certain first-generation products. We provided kinetic and mechanistic information on numerous products using a gamma kinetics parameterization fit.

We compare and contrast observed products with predictions from the Master Chemical Mechanism (MCM v3.3.1), which provides explicit representation of chemical reactions that constitute the overall aromatic oxidation mechanism on the basis of the extensive body of existing experimental work. Laboratory studies are a vital support for the model, and the agreement between these studies and the MCM output is one of the important criteria demonstrating the accuracy of the kinetic model prediction. MCM accurately predicts the overall presence and importance of the three major channels for the primary OH-initiated oxidation of aromatic compounds (peroxide-bicyclic, benzaldehyde and phenolic). However, the epoxy-oxy channel appears to be overpredicted by the kinetic model. In both systems we observed a variety of stable bicyclic products which underlines the importance of the bicyclic channel in the oxidation of aromatic compounds (Fig. 1). MCM correctly predicts the greater importance of the bicyclic pathway for the more substituted aromatics, though the speciated fate of BPRs is not entirely consistent with observations. In addition to bicyclic organonitrates, carbonyls, and alcohols, we detect numerous compounds with molecular formulas corresponding to bicyclic hydroperoxides, which suggests that this class of products may be formed in the oxidation of aromatic molecules even under high-NO conditions. Recent studies (Molteni et al., 2018; Wang et al., 2017) suggest that bicyclic peroxy radicals can undergo isomerization and autooxidation reactions leading to the formation of HOMs. Furthermore, Molteni et al. (2018) report that the HOM yields from various aromatics are relatively uniform and are not linked to bicyclic peroxy radical or phenol formation yields. Here, we observe the formation of highly oxygenated compounds with a high O:C ratio (up to 1.1) in both systems. However, the abundance of these compounds is greater in the case of 1,2,4-TMB for which the yield of bicyclic peroxy radicals is higher (Fig. 4). Moreover, the observed kinetics of these compounds suggests that they might be produced by more than one pathway, including both the isomerization/autooxidation reactions and further oxidation of phenols and benzaldehydes. Many of these compounds are low in volatility and comprise a significant fraction (more than 25%) of SOA mass. These findings emphasize the significance of ring-retaining highly oxygenated products for SOA formation and provide further evidence that isomerization and autooxidation reactions can be fast enough to compete with bimolecular reactions with NO and HO_2 even under high-NO conditions (in this study the total BPR reactivity is estimated to be ~0.1-0.2 s^{-1} (Figs. S3 and S4)). A plethora of fragmentary

https://doi.org/10.5194/acp-2019-666
Preprint. Discussion started: 7 August 2019

Atmospheric Chemistry and Physics Discussions

ring-retaining products is observed in the gas phase in both systems, many of which are not present in MCM, which underlines the importance of the fragmentation pathway in oxidation of aromatic compounds. Numerous ring scission products are detected, including C_2-C_7 dicarbonyls and $C_{4\text{-}6}H_{4\text{-}8}O_3$ products, possibly epoxydicarbonyls. The kinetics of the ring scission products (e.g., generation number *m*) is consistent between the two systems, which suggests that many of those carbonyls are produced in more than one pathway with differing number of reaction steps with OH, and those pathways are similar between different aromatic systems.

Competing interests. Authors declare no competing interests.

Author contributions. AZ, ARK, MB, JEK, KJN, CYL, JCR, JLC, JRR, and MRC collected and analysed data. ARK developed the GKP analysis. FNK and JHK provided project guidance. AZ prepared the manuscript with contributions from all co-authors.

Acknowledgments. This work was supported by the Harvard Global Institute, the NSF award AGS-1638672, and a core center grant P30-ES002109 from the National Institute of Environmental Health Sciences, National Institutes of Health. ARK acknowledges support from the Dreyfus Postdoctoral Program. MB acknowledges support from the Austrian science fund (FWF), grant J-3900.

https://doi.org/10.5194/acp-2019-666
Preprint. Discussion started: 7 August 2019

Atmospheric Chemistry and Physics Discussions

References

Arey, J., Obermeyer, G., Aschmann, S.M., Chattopadhyay, S., Cusick, R.D., and Atkinson, R.: Dicarbonyl Products of the OH Radical-Initiated Reaction of a Series of Aromatic Hydrocarbons, Environ. Sci. Technol., 43, 3, 683-689, doi: 10.1021/es8019098, 2009.

Bianchi, F., Kurtén, T., Riva, M., Mohr, C., Rissanen, M.P., Roldin, P., Berndt, T., Crounse, J.D., Wennberg, P.O., Mentel, T.F., Wildt, J., Junninen, H., Jokinen, T., Kulmala, M., Worsnop, D.R., Thornton, J.A., Donahue, N., Kjaergaard, H.G., and Ehn M.: Highly Oxygenated Organic Molecules (HOM) from Gas-Phase Autoxidation Involving Peroxy Radicals: A Key Contributor to Atmospheric Aerosol, Chem. Rev. 119 (6), 3472–3509, doi:10.1021/acs.chemrev.8b00395, 2019.

Birdsall, A.W., Andreoni, J.F., and Elrod, M.J.: Investigation of the Role of Bicyclic Peroxy Radicals in the Oxidation Mechanism of Toluene, J. Phys. Chem. A, 114, 10655-10663, doi:10.1021/jp105467e, 2010.

Birdsall, A.W., and Elrod, M.J.: Comprehensive NO-Dependent Study of the Products of the Oxidation of Atmospherically relevant Aromatic Compounds, J. Phys. Chem. A, 115, 5397-5407, doi:10.1021/jp.2010327, 2011.

Bloss, C., Wagner, V., Jenkin, M. E., Volkamer, R., Bloss, W. J., Lee, J. D., Heard, D. E., Wirtz, K., Martin-Reviejo, M., Rea, G., Wenger, J. C., and Pilling, M. J.: Development of a detailed chemical mechanism (MCMv3.1) for the atmospheric oxidation of aromatic hydrocarbons, Atmos. Chem. Phys., 5, 641-664, doi:10.5194/acp-5-641-2005, 2005

Bohn B., and Zetzsch, C: Kinetics and mechanism of the reaction of OH with the trimethylbenzenes – experimental evidence for the formation of adduct isomers, Phys. Chem. Chem. Phys., 14, 13933–13948, doi: 10.1039/c2cp42434g, 2012.

Calvert, J., Atkinson, R., Becker, K.H., Kamens, R., Seinfeld, J., Wallington, T., and Yarwood, G.: The mechanisms of atmospheric oxidation of aromatic hydrocarbons, Oxford University Press, Inc., New York, 2002.

Canagaratna, M. R., Jimenez, J. L., Kroll, J. H., Chen, Q., Kessler, S. H., Massoli, P., Hildebrandt Ruiz, L., Fortner, E., Williams, L. R., Wilson, K. R., Surratt, J. D., Donahue, N. M., Jayne, J. T., and Worsnop, D. R.: Elemental ratio measurements of organic compounds using aerosol mass spectrometry: characterization, improved calibration, and implications, Atmos. Chem. Phys., 15, 253-272, doi:10.5194/acp-15-253-2015, 2015.

DeCarlo, P.F., Kimmel, J.R., Trimborn, A., Northway, M.J., Jayne, J.T., Aiken, A.C., Gonin, M., Fuhrer, K., Horvath, T., Docherty, K.S., Worsnop, D.R., and Jimenez, J.L.: Field-Deployable, High-Resolution, Time-of-Flight Aerosol Mass Spectrometer, Anal. Chem., 78 (24), 8281-8289, doi:10.1021/ac061249n, 2006.

Galloway, M. M., Huisman, A. J., Yee, L. D., Chan, A.W. H., Loza, C. L., Seinfeld, J. H., and Keutsch, F. N.: Yields of oxidized volatile organic compounds during the OH radical initiated oxidation of isoprene, methyl vinyl ketone, and methacrolein under high-NO_X conditions, Atmos. Chem. Phys., 11, 10779–10790, doi:10.5194/acp-11-10779-2011, 2011.

Hansel, A., Scholz, W., Mentler, B., Fischer L., and Berndt, T.: Detection of RO_2 radicals and other products from cyclohexene ozonolysis with NH_4^+ and acetate ionization mass spectrometry, Atmos. Env., 186, 248–255, 5 doi:10.1016/j.atmosenv.2018.04.023, 2018.

https://doi.org/10.5194/acp-2019-666
Preprint. Discussion started: 7 August 2019

Huisman, A.J., Hottle, J.R., Coens, K.L., DiGangi, J.P., Galloway, M.M., Kammrath, A., and Keutsch., F.N.: Laser-Induced Phosphorescence for the in Situ Detection of Glyoxal at Part per Trillion Mixing Ratios, Anal. Chem., 80, 5884–5891, doi:10.1021/ac800407b, 2008.

Hu, D., Q. J. Bian, T. W. Y. Li, A. K. H. Lau, and J. Z. Yu (2008), Contributions of isoprene, monoterpenes, beta-caryophyllene, and toluene to secondary organic aerosols in Hong Kong during the summer of 2006, J. Geophys. Res.-Atmos., 113, D22206, doi:10.1029/2008JD010437, 2008

Hunter, J.F., Carrasquillo, A.J., Daumit, K.E., and Kroll J.H.: Secondary Organic Aerosol Formation from Acyclic, Monocyclic, and Polycyclic Alkanes. Environ. Sci. Technol., 48, 10227−10234, doi:10.1021/es502674s, 2014

Jenkin, M. E., Saunders, S. M., Wagner, V., and Pilling, M. J.: Protocol for the development of the Master Chemical Mechanism, MCM v3 (Part B): tropospheric degradation of aromatic volatile organic compounds, Atmos. Chem. Phys., 3, 181–193, doi:10.5194/acp-3-181-2003, 2003.

Klotz, B., Sorensen, S., Barnes, I., Becker, K.-H., Etzkorn, T., Volkamer, R., Platt, U., Wirtz, K., and Martin-Reviejo, M.: Atmospheric Oxidation of Toluene in a Large-Volume Outdoor Photoreactor: In Situ Determination of Ring-Retaining Product Yields, J. Phys. Chem. A, 102, 10289−10299 doi:10.1021/jp982719n, 1998.

Koss, A.R., Canagaratna, M., Zaytsev, A., Krechmer, J.E., Breitenlechner, M., Nihill, K.J., Lim, C.Y., Rowe, J.C., Roscioli, J.R., Keutsch, F.N., and Kroll, J.H.: Dimensionality-reduction techniques for complex mass spectrometric datasets: application to laboratory atmospheric organic oxidation experiments, Atmos. Chem. Phys. Discuss., doi:10.5194/acp-2019-469, in review, 2019.

Krechmer, J.E., Pagonis, D., Ziemann, P.J., and Jimenez, J.L.: Quantification of Gas-Wall Partitioning in Teflon Environmental Chambers Using Rapid Bursts of Low-Volatility Oxidized Species Generated in Situ, Environ. Sci. Technol. 50(11), 5757−5765, doi:10.1021/acs.est.6b00606, 2016.

Krechmer, J.E., Lopez-Hilfiker, F., Koss, A., Hutterli, M., Stoermer, C., Deming, B., Kimmel, J., Warneke, C., Holzinger, R., Jayne, J., Worsnop, D., Fuhrer, K., Gonin, M., and de Gouw J.: Evaluation of a New Vocus Reagent-Ion Source and Focusing Ion-Molecule Reactor for use in Proton-Transfer-Reaction Mass Spectrometry, Anal. Chem., 90, 20, 12011-12018, doi:10.1021/acs.analchem.8b02641, 2018.

Lopez-Hilfiker, F. D., Mohr, C., Ehn, M., Rubach, F., Kleist, E., Wildt, J., Mentel, Th. F., Lutz, A., Hallquist, M., Worsnop, D., and Thornton, J. A.: A novel method for online analysis of gas and particle composition: description and evaluation of a Filter Inlet for Gases and AEROsols (FIGAERO), Atmos. Meas. Tech., 7, 983-1001, doi:10.5194/amt-7-983-2014, 2014.

Lopez-Hilfiker, F. D., Iyer, S., Mohr, C., Lee, B. H., D'Ambro, E. L., Kurtén, T., and Thornton, J. A.: Constraining the sensitivity of iodide adduct chemical ionization mass spectrometry to multifunctional organic molecules using the collision limit and thermodynamic stability of iodide ion adducts, Atmos. Meas. Tech., 9, 1505-1512, doi:10.5194/amt-9-1505-2016, 2016.

Li, Y., and Wang, L.: The atmospheric oxidation mechanism of 1,2,4-trimethylbenzene initiated by OH radicals, Phys. Chem. Chem. Phys., 16, 17908-17917, doi:10.1039/c4cp02027h, 2014.

Li, L., Tang, P., Nakao, S., and Cocker III, D. R.: Impact of molecular structure on secondary organic aerosol formation from aromatic hydrocarbon photooxidation under low-NO_x conditions, Atmos. Chem. Phys., 16, 10793-10808, doi:10.5194/acp-16-10793-2016, 2016.

Loison, J.-C., Rayez, M.-T., Rayez, J.-C., Gratien, A., Morajkar, P., Fittschen, C., and Villenave, E.: Gas-Phase Reaction of Hydroxyl Radical with Hexamethylbenzene, J. Phys. Chem. A, 116, 12189−12197, doi:10.1021/jp307568c, 2012.

Molteni, U., Bianchi, F., Klein, F., El Haddad, I., Frege, C., Rossi, M. J., Dommen, J., and Baltensperger, U.: Formation of highly oxygenated organic molecules from aromatic compounds, Atmos. Chem. Phys., 18, 1909-1921, doi:10.5194/acp-18-1909-2018, 2018.

Nishino, N., Arey, J., and Atkinson, R.: Formation Yields of Glyoxal and Methylglyoxal from the Gas-Phase OH Radical-Initiated Reactions of Toluene, Xylenes, and Trimethylbenzenes as a Function of NO2 Concentration, J. Phys. Chem. A, 114, 10140, doi:10.1021/jp105112h, 2010.

Noda, J., Volkamer R., and Molina M.J.: Dealkylation of Alkylbenzenes: A Significant Pathway in the Toluene, *o*-, *m*-, *p*-Xylene + OH Reaction, J. Phys. Chem. A, 113, 9658–9666, doi:10.1021/jp901529k, 2009.

Olariu, R. I., Klotz, B., Barnes, I., Becker, K. H., and Mocanu, R.: FT-IR study of the ring-retaining products from the reaction of OH radicals with phenol, o-, m-, and p-cresol, Atmos. Environ., 36, 3685–3697, 2002.

Orlando, J. J. and Tyndall, G. S.: Laboratory studies of organic peroxy radical chemistry: an overview with emphasis on recent issues of atmospheric significance, Chem. Soc. Rev., 41, 6294–6317, doi:10.1039/c2cs35166h, 2012.

Praske, E., Crounse, J.D., Bates, K.H., Kurtén, T., Kjaergaard, H.G., and Wennberg, P.O.: Atmospheric Fate of Methyl Vinyl Ketone: Peroxy Radical Reactions with NO and HO_2, J. Phys. Chem. A, 119 (19), 4562–4572, doi: 10.1021/jp5107058, 2015.

Schwantes, R. H., Schilling, K. A., McVay, R. C., Lignell, H., Coggon, M. M., Zhang, X., Wennberg, P. O., and Seinfeld, J. H.: Formation of highly oxygenated low-volatility products from cresol oxidation, Atmos. Chem. Phys., 17, 3453-3474, https://doi.org/10.5194/acp-17-3453-2017, 2017.

Smith, D. F., McIver, C. D., and Kleindienst, T. E.: Primary Product Distribution from the Reaction of Hydroxyl Radicals with Toluene at ppb NOx Mixing Ratios, J. Atmos. Chem., 30, 209−228, doi:10.1023/A:1005980301720, 1998.

Smith, D.F., Kleindienst, T.E., and McIver, D.F.: Primary Product Distributions from the Reaction of OH with *m*-, *p*-Xylene, 1,2,4- and 1,3,5-Trimethylbenzene, Journal of Atmospheric Chemistry, 34, 339, doi: 10.1023/A:1006277328628, 1999.

Tang, J.H., Chan, L.Y., Chan, C.Y., Li, Y.S., Chang, C.C., Wang, X.M., Zou, S.C., Barletta, B., Blake, D.R., and Wu, D.: Implications of changing urban and rural emissions on non-methane hydrocarbons in the Pearl River Delta region of China, Atmospheric Environment, 42, 3780–3794, doi:10.1016/j.atmosenv.2007.12.069, 2007.

Wang, S., Wu, R., Berndt, T., Ehn, M., and Wang, L.: Formation of Highly Oxidized Radicals and Multifunctional Products from the Atmospheric Oxidation of Alkylbenzenes, Environ. Sci. Technol., 51 (15), 8442–8449, doi:10.1021/acs.est.7b02374, 2017.

Wolfe, G.M., Marvin, M.M., Roberts, S.J., Travis, K.R., and Liao, J.: The Framework for 0-D Atmospheric Modeling (F0AM) v3.1, Geosci. Model Dev., 9, 3309-3319, doi:10.5194/gmd-2016-175, 2016.

https://doi.org/10.5194/acp-2019-666
Preprint. Discussion started: 7 August 2019

Atmospheric Chemistry and Physics Discussions

Wu, R., Pan, S., Li, Y., and Wang, L.: Atmospheric Oxidation Mechanism of Toluene, J. Phys. Chem. A., 118, 4533-4547, doi:10.1021/jp500077f, 2014.

Wyche, K. P., Monks, P. S., Ellis, A. M., Cordell, R. L., Parker, A. E., Whyte, C., Metzger, A., Dommen, J., Duplissy, J., Prevot, A. S. H., Baltensperger, U., Rickard, A. R., and Wulfert, F.: Gas phase precursors to anthropogenic secondary organic aerosol: detailed observations of 1,3,5-trimethylbenzene photooxidation, Atmos. Chem. Phys., 9, 635-665, doi:10.5194/acp-9-635-2009, 2009.

Zaytsev, A., Breitenlechner, M., Koss, A. R., Lim, C. Y., Rowe, J. C., Kroll, J. H., and Keutsch, F. N.: Using collision-induced dissociation to constrain sensitivity of ammonia chemical ionization mass spectrometry (NH_4^+ CIMS) to oxygenated volatile organic compounds, Atmos. Meas. Tech., 12, 1861-1870, doi:10.5194/amt-12-1861-2019, 2019.

Zheng, J., Shao, M., Che, W., Zhang, L., Zhong, L., Zhang, Y., and Streets, D.: Speciated VOC emission inventory and spatial patterns of ozone formation potential in the Pearl River Delta, China, Environ. Sci. Technol., 43 (22), 8580–8586, doi:10.1021/es901688e, 2009.

https://doi.org/10.5194/acp-2019-666
Preprint. Discussion started: 7 August 2019

Atmospheric Chemistry and Physics Discussions

Table 1: Major toluene oxidation products measured by PTR-MS and NH_4^+ CIMS.

Product Name	Product Formula	Generation parameter *m*	Kinetic parameter *k* (cm^3 $molecule^{-1}$ s^{-1})	Yield (%)
glyoxal	$C_2H_2O_2$	1.2	$1.3 \cdot 10^{-11}$	28%
methylglyoxal	$C_3H_4O_2$	1.3	$1.1 \cdot 10^{-11}$	15%
butenedial	$C_4H_4O_2$	0.8	$2 \cdot 10^{-11}$	8%
methylbutenedial	$C_5H_6O_2$	0.7	$2 \cdot 10^{-11}$	37%
epoxybutanedial	$C_4H_4O_3$	1.3	$1 \cdot 10^{-11}$	5%
methylepoxybutanedial	$C_5H_6O_3$	1.3	$1 \cdot 10^{-11}$	5%
benzaldehyde	C_7H_6O	1	$1 \cdot 10^{-11}$	9%
cresol	C_7H_8O	1	$2.3 \cdot 10^{-11}$	10%
dicarbonylepoxide	$C_7H_8O_3$	0.9	$2.2 \cdot 10^{-11}$	1%

Table 2: Major 124-TMB oxidation products measured by PTR-MS and NH_4^+ CIMS

Product Name	Product Formula	Generation parameter *m*	Kinetic parameter *k* (cm^3 $molecule^{-1}$ s^{-1})	Yield (%)
methylglyoxal	$C_3H_4O_2$	1.3	$1.8 \cdot 10^{-11}$	25%
biacetyl	$C_4H_6O_2$	1.3	$2.2 \cdot 10^{-11}$	10%
methylbutenedial	$C_5H_6O_2$	0.7	$3.5 \cdot 10^{-11}$	5%
dimethylbutenedial	$C_6H_8O_2$	0.9	$4.1 \cdot 10^{-11}$	40%
trimethylbutenedial	$C_7H_{10}O_2$	1	$5.1 \cdot 10^{-11}$	2%
methylepoxybutanedial	$C_5H_6O_3$	1.8	$1.9 \cdot 10^{-11}$	N/A
dimethylepoxybutanedial	$C_6H_8O_3$	1.1	$2.4 \cdot 10^{-11}$	2%
dimethylbenzaldehyde	$C_9H_{10}O$	1	$1.4 \cdot 10^{-11}$	3%
trimethylphenol	$C_9H_{12}O$	1	$3.5 \cdot 10^{-11}$	2%
dicarbonylepoxide	$C_9H_{12}O_3$	1	$4 \cdot 10^{-11}$	1%

5

https://doi.org/10.5194/acp-2019-666
Preprint. Discussion started: 7 August 2019

Atmospheric Chemistry and Physics Discussions

Table 3: Kinetics fit of gas-phase highly oxygenated compounds detected in toluene (top five rows) and 1,2,4-TMB (bottom seven rows) oxidation experiments.

Product Formula	Generation parameter *m*	Kinetic parameter *k* (cm^3 $molecule^{-1}$ s^{-1})
$C_7H_8O_4$	1.5	$1 \cdot 10^{-11}$
$C_7H_{10}O_5$	1.5	$1 \cdot 10^{-11}$
$C_7H_8O_6$	1.6	$1.1 \cdot 10^{-11}$
$C_7H_9NO_6$	2.1	$0.8 \cdot 10^{-11}$
$C_7H_9NO_8$	2	$0.9 \cdot 10^{-11}$
$C_9H_{12}O_4$	1.5	$1.8 \cdot 10^{-11}$
$C_9H_{14}O_4$	1.6	$1.7 \cdot 10^{-11}$
$C_9H_{14}O_5$	1.8	$1.9 \cdot 10^{-11}$
$C_9H_{12}O_6$	1.8	$1.4 \cdot 10^{-11}$
$C_9H_{13}NO_6$	1.4	$1.7 \cdot 10^{-11}$
$C_9H_{13}NO_7$	2.1	$2.3 \cdot 10^{-11}$
$C_9H_{13}NO_8$	2.3	$1.8 \cdot 10^{-11}$

https://doi.org/10.5194/acp-2019-666
Preprint. Discussion started: 7 August 2019

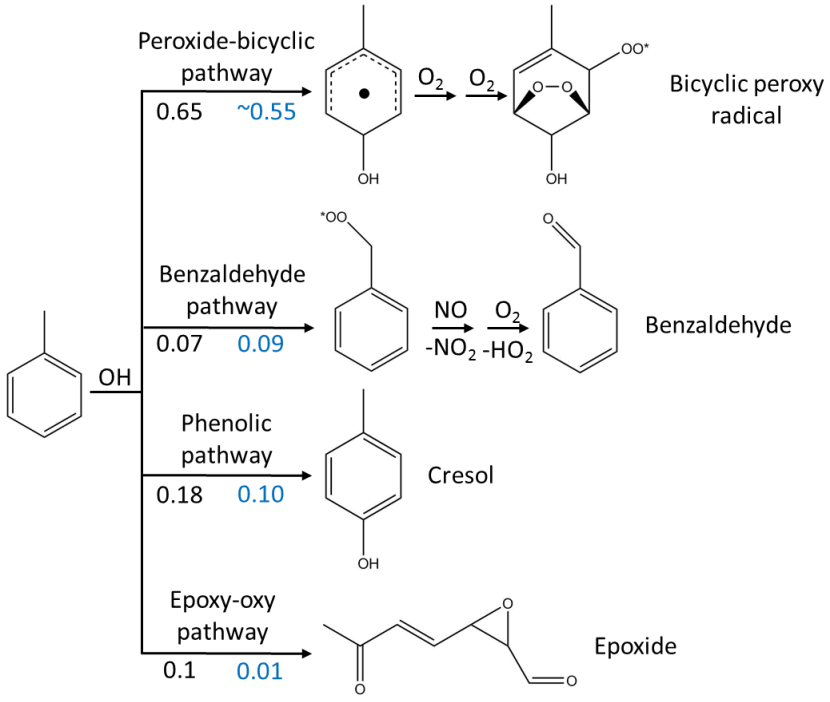

Figure 1: Gas-phase chemical mechanism for toluene photooxidation. Reaction yields for the major oxidation pathways recommended by MCM v3.3.1 are shown in black. The proposed yields from the present study are shown in blue. The yield of the peroxide-bicyclic pathway is calculated based on the yields of ring-scission products.

https://doi.org/10.5194/acp-2019-666
Preprint. Discussion started: 7 August 2019

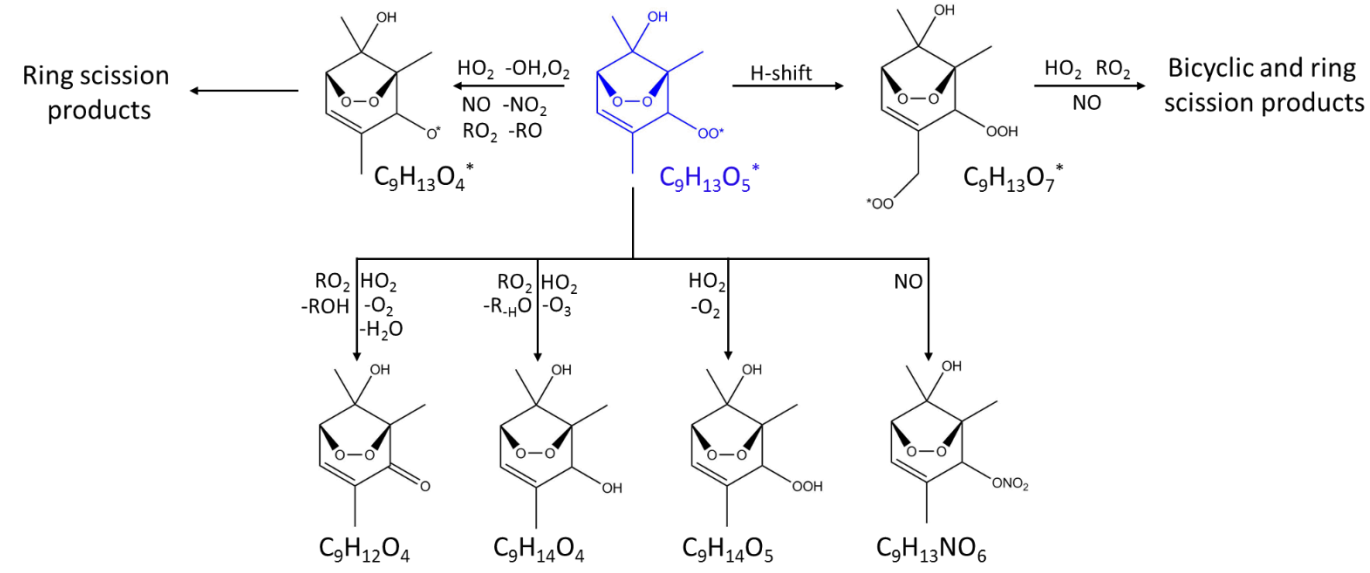

Figure 2: Oxidation pathways of bicyclic peroxy radicals in the OH-initiated oxidation of 1,2,4-trimethylbenzene. The starting radical us shown in blue.

https://doi.org/10.5194/acp-2019-666
Preprint. Discussion started: 7 August 2019

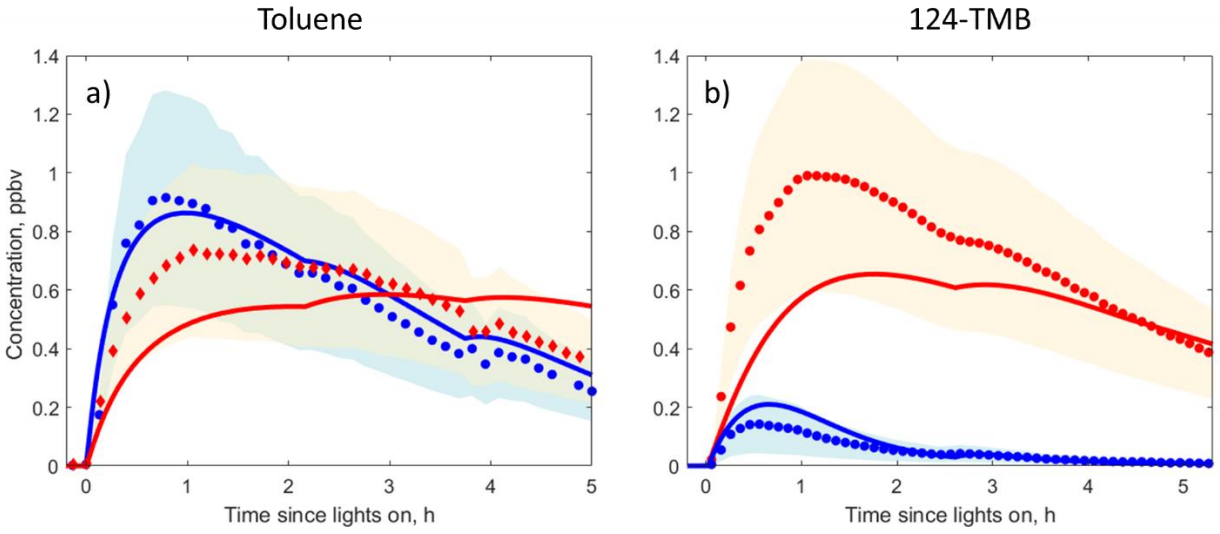

Figure 3: MCM v3.3.1 predictions (solid lines) compared to PTR-MS (circles) and NH_4^+ CIMS (diamonds) measurements under high-NO_x oxidation of (a) toluene and (b) 124-TMB for phenols (red) and benzaldehydes (blue). The uncertainty in the PTR-MS and NH_4^+ CIMS measurements is shown in blue and red shading.

https://doi.org/10.5194/acp-2019-666
Preprint. Discussion started: 7 August 2019

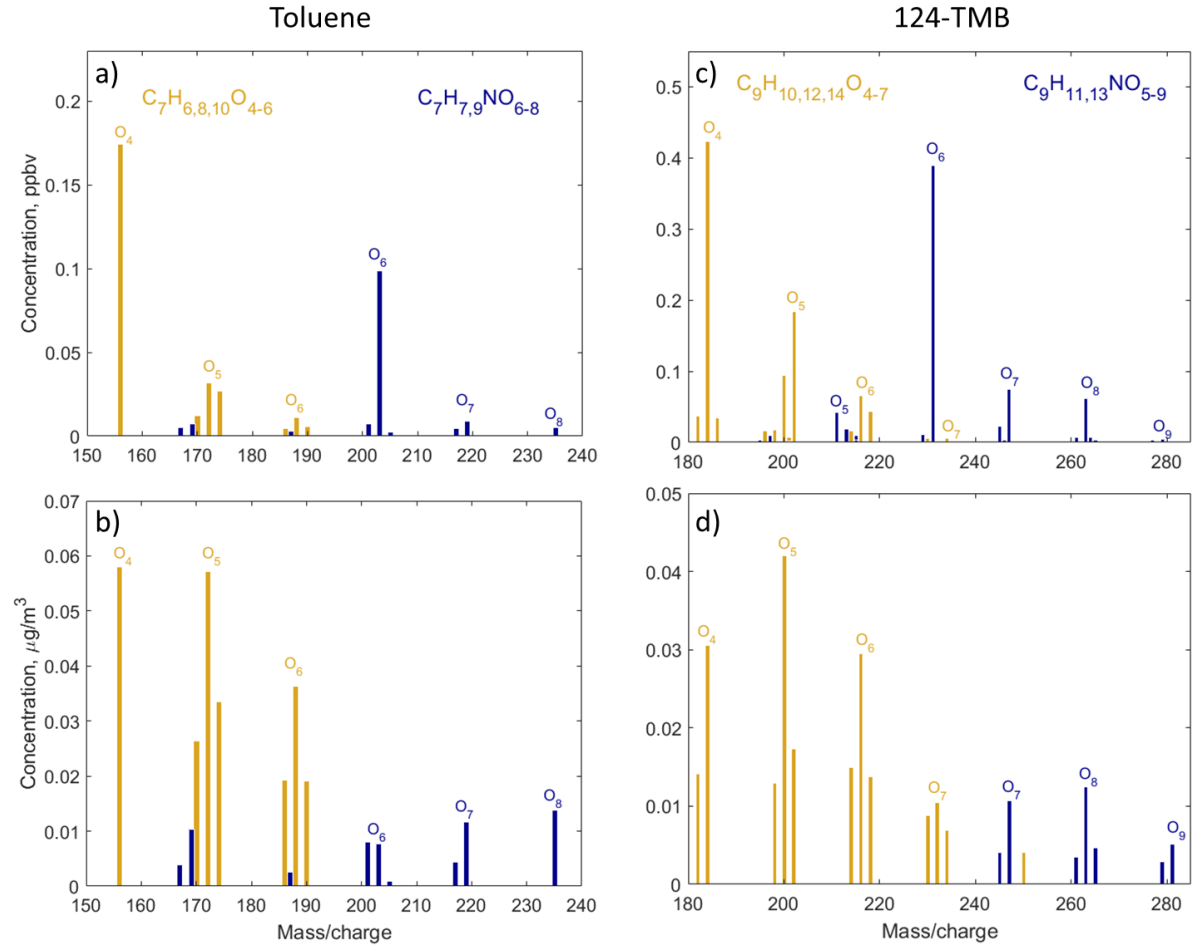

Figure 4: Mass spectra of compounds with high oxygen content (O:C > 0.44) from toluene (panels a and b) and 1,2,4-trimethylbenzene (panels c and d) detected by NH_4^+ CIMS. Gas-phase mass spectra are shown in the upper panels (a) and (c), and particle-phase mass spectra are shown in bottom panels (b) and (d). Non-nitrogen-containing compounds are shown in yellow, and nitrogen-containing compounds are shown in blue.

https://doi.org/10.5194/acp-2019-666
Preprint. Discussion started: 7 August 2019

Atmospheric Chemistry and Physics Discussions

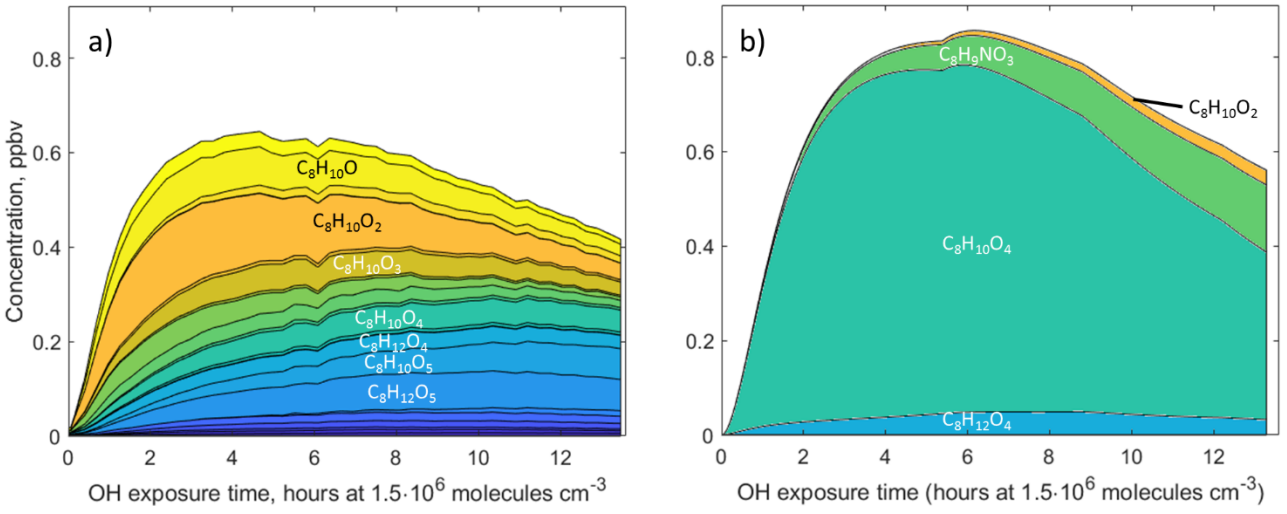

Figure 5: C_8 gas-phase products (a) detected by PTR-MS and NH_4^+ CIMS and (b) predicted by MCM v3.3.1 during oxidation of 1,2,4-trimethylbenzene.

https://doi.org/10.5194/acp-2019-666
Preprint. Discussion started: 7 August 2019

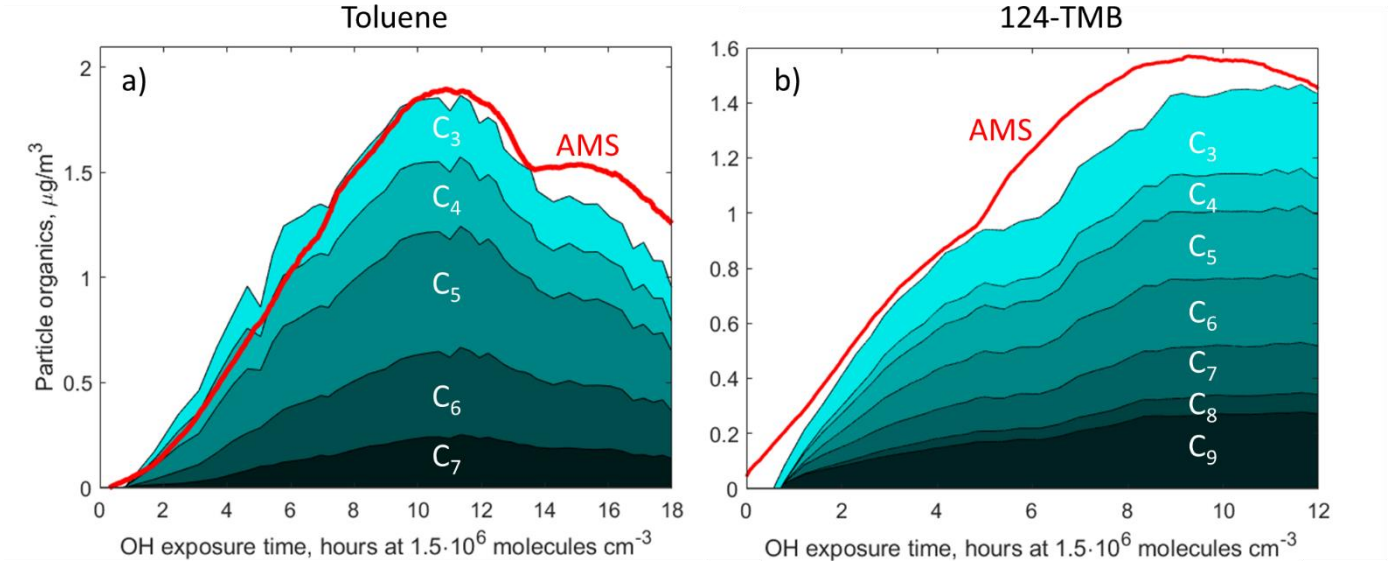

Figure 6: Total organics measured in the particle phase by NH_4^+ CIMS and binned by the carbon atom number (a) in the 124-TMB photooxidation experiment and (b) the toluene photooxidation experiment. Total carbon measured by AMS is in red.